Applied Chemical Engineering (2024) Volume 7 Issue 4 ISSN: 2578-2010 (O)
doi: 10.59429/ace.v7i4.5577

RESEARCH ARTICLE

Numerical study of the influence of flow control methods on the efficiency of a micro-gas turbine

S.K Osipov, V.P Sokolov, I.A Milyukov, M.M Shaikh , A.N Bukanov

Department of Innovative Technologies for High-Tech Industries, National Research University "Moscow Power Engineering Institute", Moscow, 111250, Russia

***Corresponding author:** Muhammad Maaz Shaikh. Email: sheykhm@mpei.ru

ABSTRACT

This paper presents innovative solutions to enhance the aerodynamic performance of the radial turbine and the efficiency of the Capstone C30 micro-gas turbine unit (micro-GTU) through the integration of a cycle air cooling system and advanced flow control mechanisms. The study investigates various flow control methods within the blade channels of the radial turbine, including splitters, triangular root fins, and inter-tier partitions. The results show that using splitters with a relative length of 0.7 increases internal relative efficiency from 80.9% to 81.75%, implementing triangular root fins enhances efficiency from 80.9% to 81.44%, and adding an inter-tier partition improves internal relative efficiency from 80.9% to 81.7%. A finned turbine configuration with splitters of relative length 0.7 achieves the highest internal relative efficiency of 82.2%. These advancements contribute to improved turbine performance and efficiency, addressing the need for enhanced domestic energy solutions in the context of distributed energy generation in Russia.

Keywords: micro gas turbine; flow simulation; efficiency of micro gas turbine; splitters & fins in radial turbine; Capstone C30 micro gas turbine

ARTICLE INFO

Received: 29 November 2024
Accepted: 20 December 2024
Available online: 27 December 2024

COPYRIGHT

Copyright © 2024 by author(s).
Applied Chemical Engineering is published by Arts and Science Press Pte. Ltd. This work is licensed under the Creative Commons Attribution-NonCommercial 4.0 International License (CC BY 4.0).
https://creativecommons.org/licenses/by/4.0/

1. Introduction

The state of distributed energy in Russia, highlighting the presence of various energy generation technologies such as gas turbine units (GTU), gas piston units (GPU), diesel power plants (DPP), microturbines, and renewable energy sources (RES). Currently, small-scale generation accounts for less than 2.3% of electricity production in Russia, significantly lower than the 10-15% seen in some Western European countries.

Distributed energy offers benefits like increased energy efficiency, reduced electricity transportation costs, smarter tariffs, and enhanced control over energy resources. However, barriers such as an inadequate legislative framework and high capital investment costs hinder the growth of small generation entities in the Russian market. Micro gas turbine units (MGTU) are increasingly used for heat and electric supply in small enterprises, yet their adoption in Russia remains limited, primarily relying on imported units.

Capstone Turbine Corporation is a leading manufacturer of microturbines, with its C30 model noted for compactness and efficiency. Challenges in the Russian market include limited technical documentation for maintenance and repair. To address this, reverse engineering of Capstone C30 components is proposed to facilitate the production of domestically sourced parts[1].

The Capstone C30 gas turbine is a modular system for generating electrical energy as a backup or prime power source. It has a high electrical efficiency of 26%, a long service life of 60,000 hours, and low emissions. The system uses natural gas as fuel and operates on a principle of air compression, heating, and expansion to generate power. The Capstone C30 has a power output of 30 kW, an electrical efficiency of 28%, and an overall efficiency of 80% in cogeneration mode. It has a compact design, weighing 478 kg and measuring 1900 x 714 x 1344 mm. The system has a low noise level of 58 dB and emits less than 9 ppmv of NOx. The Capstone C30 system consists of a compressor, recuperator, combustor, turbine, and permanent magnet generator, with a single shaft supported by air bearings that rotate at speeds up to 96.000 rpm. The system does not require oils, lubricants, coolants, or other hazardous materials, and has a simple design with minimal moving parts.

Capstone C30 system includes a compressor, recuperator, combustor, turbine, and permanent magnet generator (**Figure 1**). The rotating components are mounted on a single shaft supported by patented air bearings that rotate at speeds up to 96.000 rpm. This is the only moving part of the microturbine. The generator is cooled by the incoming air flow. The system does not use oils, lubricants, coolants, or other hazardous materials, nor does it require pumps, gearboxes, or other mechanical subsystems[2].

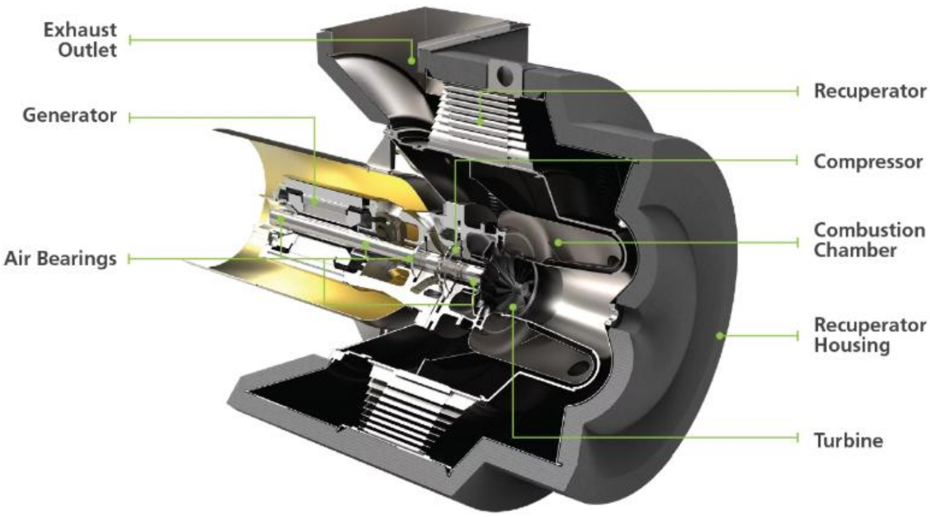

Figure 1. Capstone gas microturbine design C30.[3]

In recent decades, energy security and sustainable development issues have become increasingly important at the global level. One of the key areas in this area is the development of decentralized energy. Decentralized energy systems help to increase the reliability of energy supply, reduce energy transmission losses, and improve the environmental situation through the use of renewable energy sources and modern technologies.

One of the promising types of power plants for distributed energy are microturbine plants (micro-GTU). These plants have a number of advantages, such as high efficiency, low operating costs, the ability to operate on various types of fuel and compact dimensions.

At the moment, there are no domestic micro-GTUs on the Russian market, which creates dependence on foreign manufacturers and technologies. In this regard, active work is underway on reverse engineering of micro-GTUs, such as the Capstone units.

One of the main tasks of reverse engineering is to ensure efficiency indicators at the level of foreign analogues, as well as the desire to improve them. To increase the efficiency of micro-GTU, it is proposed improvement in the flow part of the micro-GTU, in particular the development of solutions to increase the efficiency of the radial wheel.

The following tasks are solved:

1. Conducting design calculations for a radial turbine with optimization of the flow path geometry;
2. Conducting gas-dynamic studies of the operation of a radial turbine with the addition of components to improve its aerodynamic performance;
3. Develop recommendations for improving the performance of the Capstone radial turbine C 30.

2. Literature review

2.1. Review of design calculation methods for a radial turbine

A radial flow turbine is a turbine in which the working fluid flows radially relative to the shaft. Therefore, this is the main difference between axial and radial turbines due to the direction of fluid flow in their components. In a radial turbine, the flow is smoothly oriented perpendicular to the axis of rotation and drives the turbine. This leads to lower mechanical and thermal stresses (especially when working with a hot working fluid), which allows the radial turbine to be simpler, more durable and more efficient (with a comparable power range) compared to axial turbines. However, for large power ranges (more than 5 MW), radial turbines are no longer competitive (due to heavy and expensive rotors), and their efficiency is the same as that of axial turbines.

The internal flow radial turbine has a wide range of power generation, mass flow rate and rotation speed. It can be used in huge hydroelectric power plants producing hundreds of megawatts, as well as in small closed-loop gas turbines to produce a few kilowatts of power.

These turbines were also of interest for use in Brayton cycles for spacecraft, and the National Aeronautics and Space Administration conducted many studies of radial turbines in the 1960s. NASA's studies included analytical studies of geometry, calculation of flow velocities, and other characteristics. For these turbines, efficiencies ranged from 85% to 90% for a wide range of Reynolds numbers.

The radial configuration of the blades attached to a hub, which may be cast or forged as a unit, makes these machines relatively simple to manufacture and provides increased rigidity, which contributes to the dynamic stability of the rotor as a whole[4]. This inherent stability makes radial flow turbines particularly attractive for use with high working fluid densities, such as in supercritical cycles, where relatively higher blade loading is expected.

2.2. Analysis of the flow structure in a radial impeller

When gas flows in the working wheels, a number of losses occur, which can be divided into: profile, end, edge, in the gap between the blades and the casing, disk. Profile losses are associated with the formation of a boundary layer on the surfaces of the blades. Their magnitude depends on the shape of the working blades and the meridional contours, which affect the distribution of speeds along the contours of the profiles. With a general confusor nature of the flow, in an unfavorable case, areas with a large local. The results of the conducted variable aerodynamic calculation of the radial turbine allow us to conclude that with an increase in the ratio of the radial wheel diameters, the height of the working blade at the inlet to the inner blade channel decreases. It is worth noting that the height of the nozzle blade depends on the height of the working blade at the inlet, the value of which cannot be lower than 12 mm. When the height of the blades decreases below 12 mm, the end vortices close, which leads to a sharp increase in the end energy losses in the inner blade channel and, accordingly, to a decrease in the internal relative efficiency of the radial turbine.

When rotating, the blades pass these areas with a disturbed flow, thereby creating a new vortex at their tip. At the top of the blade at the rotor inlet, the tip vortex breaks away from the blade and moves toward the exit from the inner blade channel. This creates a vortex motion in the flow part of the radial turbine. In the inner blade channel of the rotor, the separated tip vortex merges with the gas flow[5].

2.3. Review of methods for increasing the aerodynamic efficiency of a radial turbine

The complex flow in the flow section of a radial turbine is caused by the geometry of the wheel itself and is combined with strong secondary flows that are localized near the channel walls. The interaction of the turbulent boundary layer with the wheel walls affects the development of the boundary layer and causes energy losses due to surface friction resistance. Surface roughness is one of the important factors influencing the flow in the boundary layer.

This paper investigates the effect of V -shaped fins and their number on the losses inside the microturbine wheel. The development of fins with a height of no more than 0.1 mm became possible with the introduction of 3D printing of radial turbine components with various alloys of alloy steels into mechanical engineering. Other studies have shown that smooth surfaces do not always have less resistance than rough ones[6]. The fins are surface structures on the wheel hub, located in the direction of the gas flow, which help to reduce the shear stress at the hub itself. In a study of various shapes of protrusions aimed at reducing resistance on a flat plate surface, the V -shaped rib shape showed the greatest effect, reducing resistance by 8%.

3. Methodology

The geometry of the radial turbine was created based on **Table 1**.

Table 1. Geometric dimensions of the nozzle ring and wheel of a radial turbine.

Parameter	Designation	Recommended range	Dimension	Unit
Mass flow rate in turbine	G	-	0,307	kg/s
Wheel inlet diameter	D_1	-	0,1197	m
Height of blades at wheel inlet	b_1	-	0,0115 m	m
Height of nozzle ring blades	b_c	(0,9-1,0) $\cdot b_1$	0,0115	m
Inner diameter of the nozzle crown	D_c	(1,08-1,12) $\cdot D_1$	0,134	m
Nozzle crown outer diameter	D_0	(1,35-1,5) $\cdot D_1$	0,178	m
Wheel width	B_T	(0,3-0,35) $\cdot D_1$	0,0418	m
Number of wheel blades	z_l	12-18	15	-
Turbine wheel outlet outer diameter	D_2	(0,85- 0,9) $\cdot D_1$	0,1029	m
Wheel hub diameter at output	d_2	(0,25-0,32) $\cdot D_1$	0,0359	m

The calculation domain included one segment with a turbine blade. Using ANSYS Vista RTD created a solid geometry of the radial wheel, according to the parameters calculated earlier. Then ANSYS was used Workbench for creating the computational grid for the gas flow. CFD calculations were performed using ANSYS CFX 2021 R 2, boundary conditions are given in **Table 2**.

The computational grid for the inner blade channel flow volume was built in ANSYS Workbench. In this case, recommendations for choosing the parameters of the computational grid were taken into account, which, in the numerical study of hydro gas dynamic flows in typical channels of flow parts of power equipment, allow obtaining the results of a numerical experiment that deviate least from the results of a physical experiment[7]. Thus, when constructing the computational grid in the wall layer zone, a prismatic cell type with a parameter y += 5 was used with a number of prismatic layers of at least 8. These parameters of the prismatic grid were chosen to obtain adequate results when modeling using the RANS (Reynolds - averaged Navier-Stokes) with SST turbulence model[8-10]. The main flow zone is formed from tetrahedrons, the maximum linear size of the main cell in the flow was 1 mm[11]. The constructed computational grid for the flow volume of the working channel is shown in **Figure 2**.

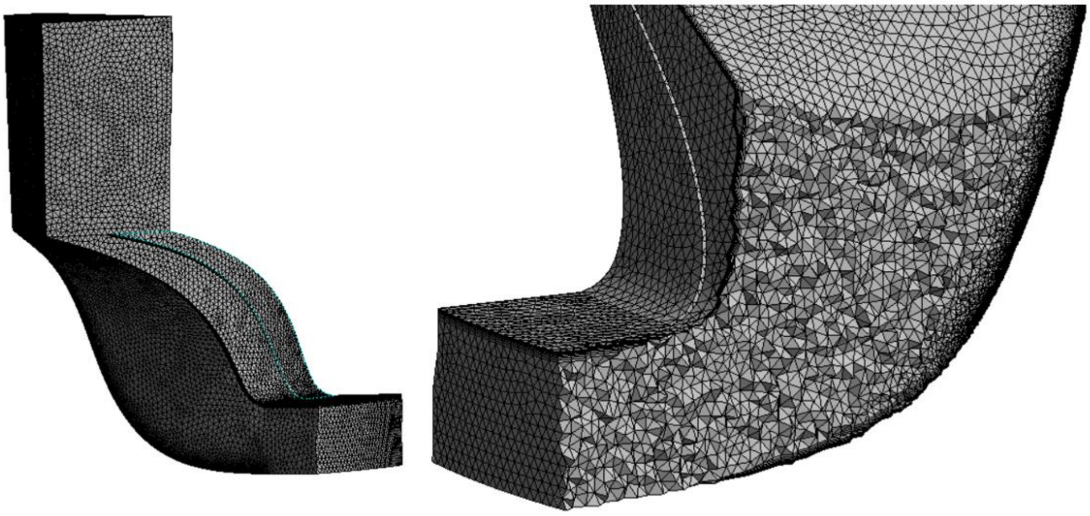

Figure 2. Calculated surface and volume mesh of the inner blade working channel.

Table 2. Parameters and boundary conditions for calculating a radial turbine.

Turbine entrance	
Pressure, kPa	241.01
Temperature, K	1143.15
Consumption, kg /s	0.307
Turbine exit	
Pressure, kPa	103

4. Result and discussion

Thus, to increase the aerodynamic efficiency of the turbine's inner blade radial channels, splitters of various lengths were added to the wheel geometry **Figure 3**.

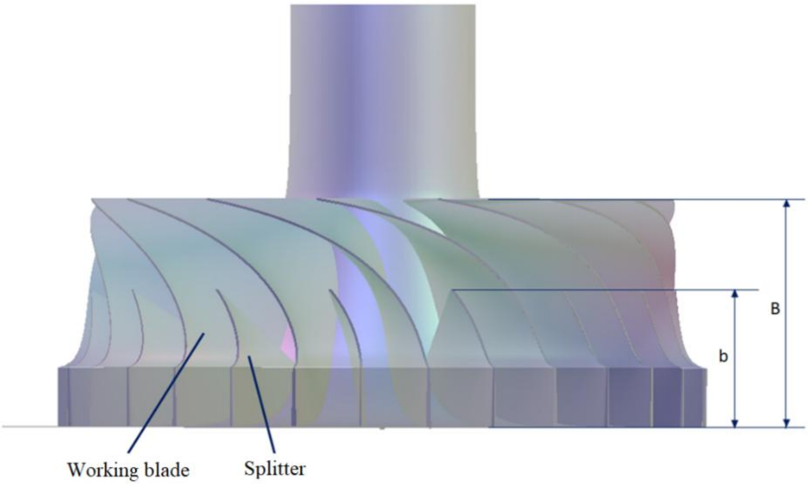

Figure 3. Radial wheel with splitters.

Adding splitters (separating blades) is one of the ways to increase the aerodynamic efficiency of a radial turbomachine. The splitter profile follows the profile of the working blade, but its length along the flow path can vary.

To determine the effect of splitters on turbine efficiency, simulations were performed with three geometry variants. Each geometry differed in the relative length of the splitters b/B.

Figure 4 shows the structure of the flow lines of the flow region without splitters and with splitters of different relative lengths b/B = 0.3; 0.5; 0.7.

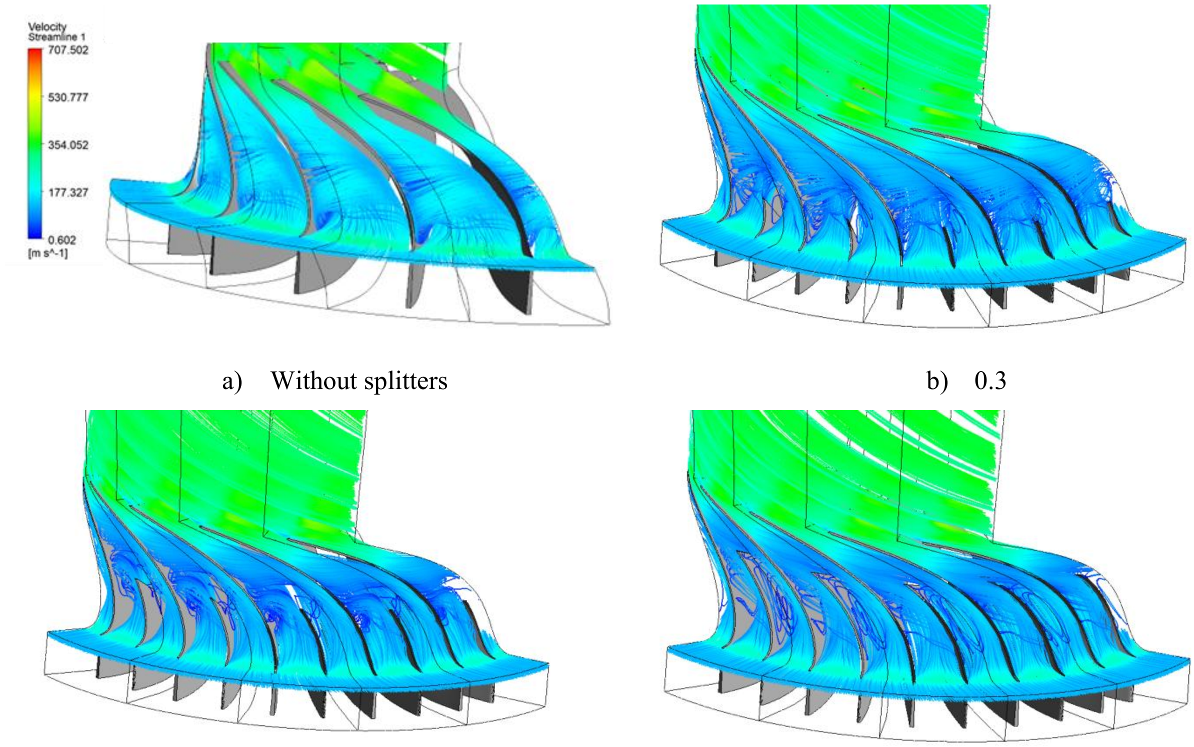

a) Without splitters

b) 0.3

c) 0.5

d) 0.7

Figure 4. Flow structure with different relative splitter lengths.

Analysis of the results shows that the installation of splitters made it possible to divide a large peripheral vortex, thereby preventing the flow of working gas from one blade to another. Quantitative processing of the splitter modeling results is presented in **Table 3**.

Table 3. Quantitative processing of flow simulation in a radial turbine.

Speed, m/s		Temperature, K		Pressure, Pa		Enthalpy, kJ/kg	
inlet	outlet	inlet	outlet	inlet	outlet	inlet	outlet
Turbine without splitters							
207.276	580.267	1143.15	983.985	222284	112131	1338.32	1061.5
Splitters 0.7							
207.276	567.646	1143.15	981.539	225939	117695	1338.32	1059.01
Splitters 0.5							
207.276	565.563	1143.15	982.658	225977	117817	1338.32	1059.18
Splitters 0.3							
206.496	565.344	1143.15	982.797	226051	117835	1338.32	1059.52

The final increase in the internal relative efficiency was 0.85% with a relative splitter length of b/B=0,7. With an increase in the relative length of the separator blade, the region of low speeds at the root of the main blade of the radial wheel decreases, which is also the reason for the increase in the turbine efficiency. The turbine efficiency with varying splitter lengths is shown in **Figure 5**.

An example of calculating the relative internal efficiency of a turbine is given for a variant with a relative splitter length b/B=0,7:

$$\eta_{oi} = \frac{G \cdot (h_0 - h_k)}{G \cdot (h_0 - h_{kt})} = \frac{0{,}307 \cdot (1338{,}32 - 1059{,}01)}{0{,}307 \cdot (1338{,}32 - 996{,}65)} \cdot 100 = 81.75\%$$

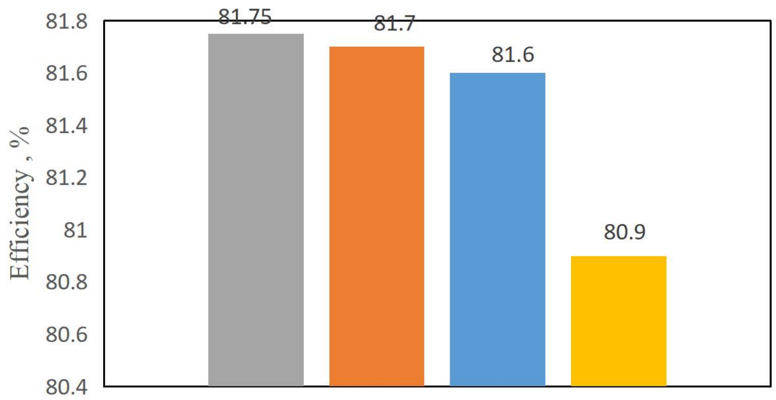

Figure 5. Efficiency of different splitter configurations compared to a basic radial turbine. Splitter length 0.7 (81.75%), Splitter length 0.5 (81.7%), Splitter length 0.3 (81.6%) and Without splitter (80.9%)

To analyze the effect of the inter-tier partition on the unevenness of the velocity field in the working channel of the radial turbine, two planes transverse to the flow were constructed (**Figure 6**). The position of the first plane was chosen at the point where the root flow flowing down the convex surface begins to twist into a vortex cord. The second plane is located closer to the outlet from the working wheel.

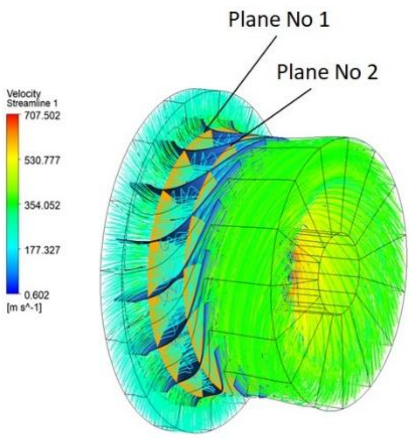

Figure 6. Location of control planes for analysis of the velocity field non-uniformity in the working channel of a radial turbine.

The velocity fields in the transverse planes of a traditional turbine wheel and a two-tier turbine wheel are shown in **Figures 7** and **8**.

The analysis of the results shows that the installation of an inter-tier partition allows to reduce the unevenness of the velocity field in the inter-blade channels of the radial wheel. Thus, in plane No. 1, when installing an inter-tier partition, the area of increased velocities on the periphery of the convex part of the working blade was eliminated (**Figure 6**). It is worth noting that the local increase in speed in this area is due to the fact that part of the root flow flowing down the surface of the blade is added to the main flow on the periphery of the working wheel. At the same time, closer to the outlet section, the area with a local increase in speed becomes larger (**Figure 7a**), which is due to the increase in the flow rate of the flow that flows from other parts of the channel to the peripheral zone.

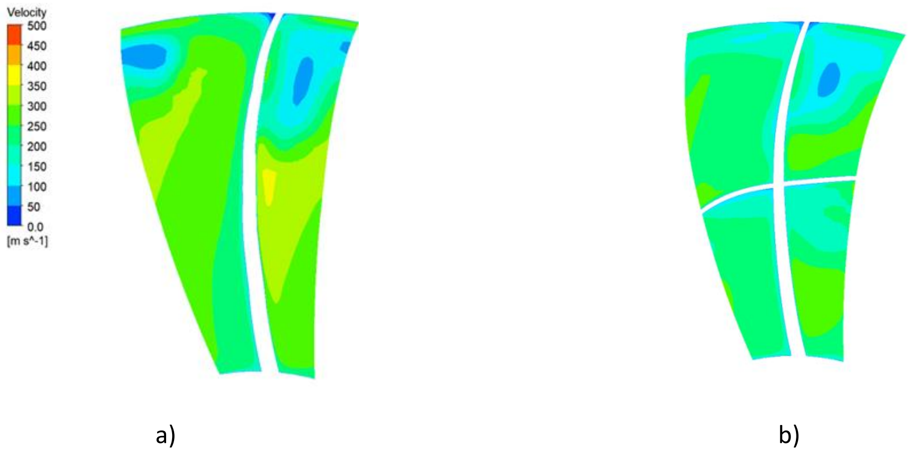

Figure 7. Velocity field in plane No. 1 of the channel of the working radial wheel a) traditional impeller b) Two-tier impeller.

a) b)

Figure 8. Velocity field in plane No. 2 of the channel of the working radial wheel a) Traditional impeller b) Two-tier impeller.

When splitters are added to the design of a two-tier radial wheel, the unevenness of the velocity field in the cross section increases. A stagnation zone appears, which is associated with a decrease in the cross-sectional area of the channel at the outlet of the radial turbine, which significantly reduces the efficiency of the turbine (**Figure 10**).

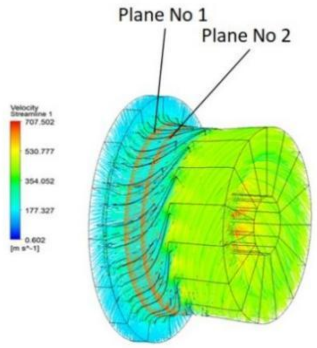

Figure 9. Location of control planes for analysis of velocity field non-uniformity in the working channel of a radial turbine with splitters.

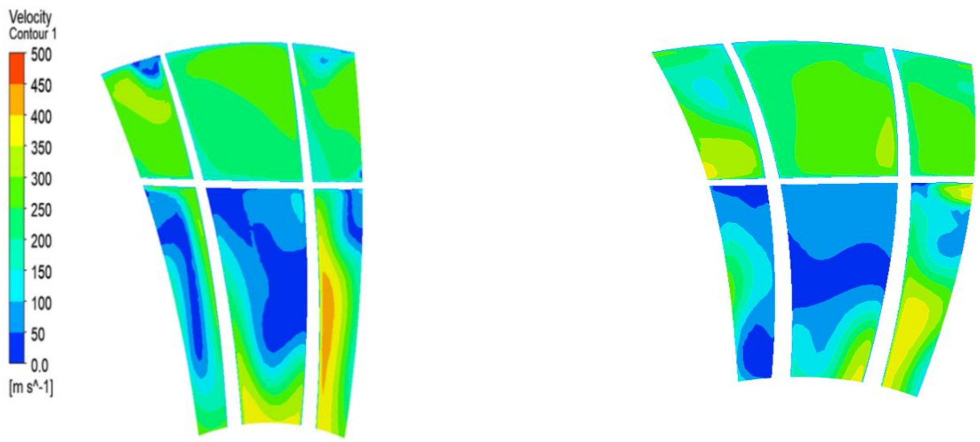

a) Velocity field in plane No. 1 b) Velocity field in plane No. 2

Figure 10. Velocity field in the transverse plane of a two-tier channel of a working radial wheel with the addition of splitters.

Adding an inter-tier partition without splitters to the turbine wheel prevents flow transfer to the periphery and, accordingly, reduces the unevenness of the velocity field in the inter-blade channel, which leads to an increase in the internal relative efficiency of the flow path by 0.8%.

The computational grid was refined in the area of fin placement due to their small size. A boundary layer was also created at the root, on the periphery and on the blade. The temperature and pressure of the gas were set at the turbine inlet, and only the pressure at the outlet. Also, due to the use of a flow segment in a radial turbine, a periodicity condition in the radial direction with a boundary condition of wheel rotation was imposed on the planes formed by the section[12].

To evaluate the mechanism of the fins, the flow structure between the finned (6 fins) and smooth radial wheel hubs is compared. The transverse flow interacts with the protrusions on the hub surface, impeding its movement and creating secondary vortices that prevent the longitudinal vortex from moving between the fins. The streamlines in **Figure 11** reflect a strong transverse fluid flow on the hub surface. The introduction of fins on the hub surface forms an obstacle that slows down the transverse movement and straightens the flow in the longitudinal direction.

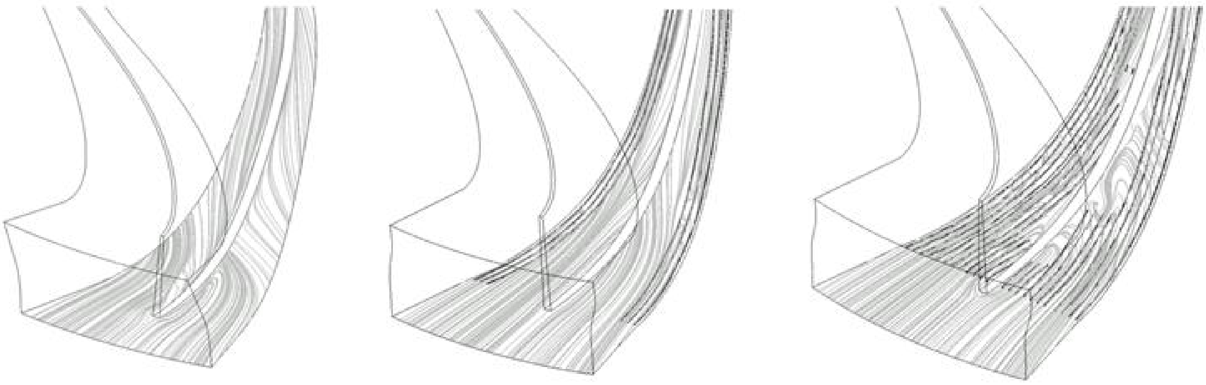

a) Without fins b) With partial finning c) Fully finned

Figure 11. Streamlines in the root section.

The vorticity above the fin is slightly higher due to the secondary vortices generated at the tip of each fin, as shown in **Figure 12**. The vorticity reaches its maximum value near the tip, where the secondary vortices are located. However, the secondary vortex near the fin tip does not have a significant effect on the drag increase, since the vortex size is relatively small and it interacts with a very small area[13]. **Figure 13** shows the CFD results for the 8-fin and 4-fin configurations.

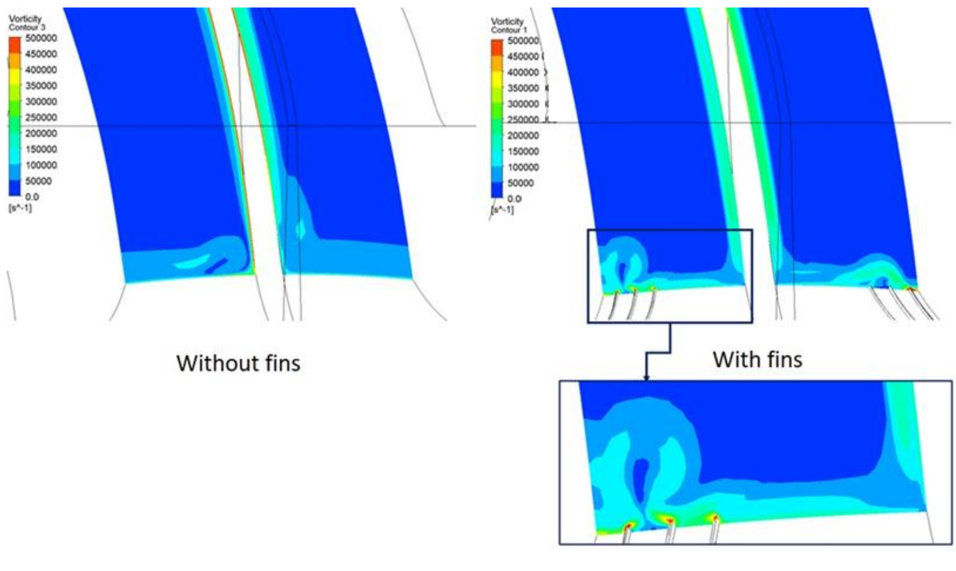

Figure 12. Structure of the root vortex in a radial wheel with and without 6 fins.

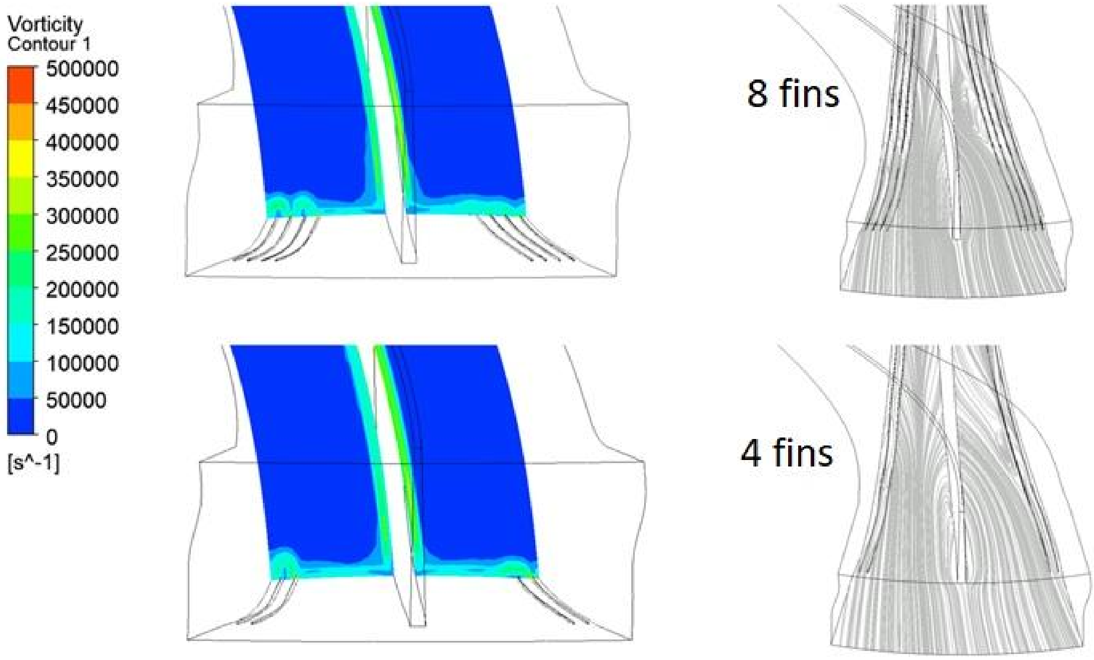

Figure 13. Vorticity diagram in the channel and flow lines on the hub.

To evaluate the effect of increasing fin tip vorticity on the wall shear stress[14], wall shear stress values were taken (wall shear stress) from a plane located 43.1 mm from the flow inlet. The shear stress graph (**Figure 14**) at the root section shows that increasing vorticity at the fin tips increases the wall shear stress in small areas around the tips, while the shear stress between the fins decreases, keeping the average value lower than for a smooth surface. Wall shear stress directly affects losses with the formation of a boundary layer on the surface of the wheel hub[15]. Finning allows minimizing the average wall shear stress over the area of the flow path.

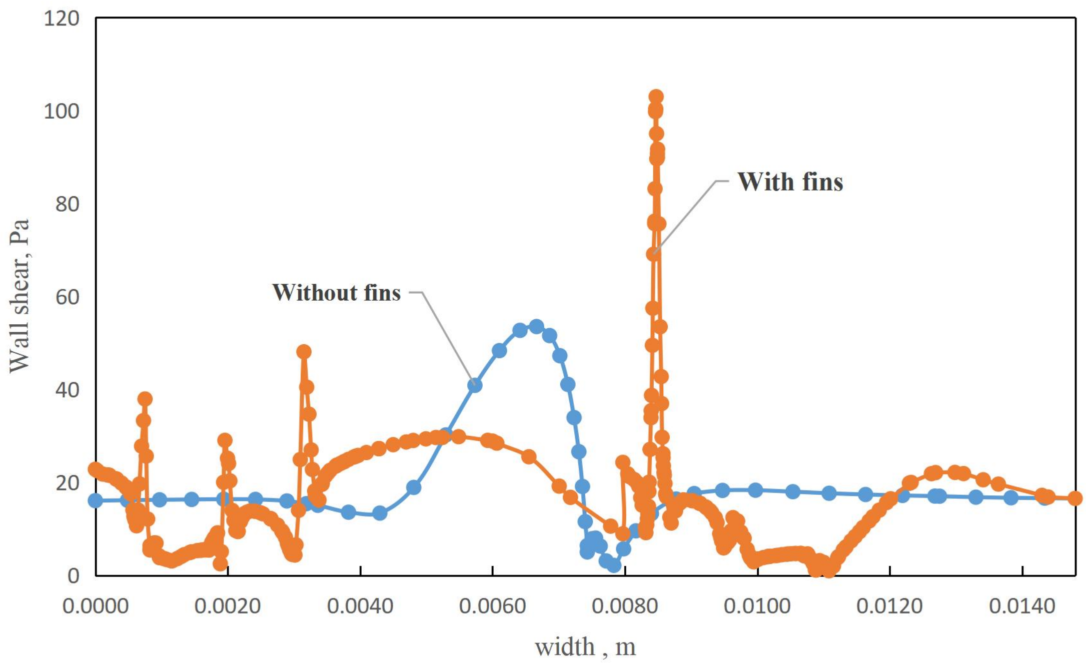

Figure 14. Dependence of shear stress on channel width at the level of the fins.

The results in **Table 6** show that increasing the number of fins in the channel reduces the average value of the shear stress at the hub. However, the increase in efficiency slows down when more than 8 fins are added to the channel and results in a slight increase in the efficiency of the turbine wheel.

An example of calculating the relative internal efficiency of a turbine is given for a variant with 4 fins:

$$\eta_{oi} = \frac{G \cdot (h_0 - h_k)}{G \cdot (h_0 - h_{kt})} = \frac{0.307 \cdot (1338.32 - 1061.47)}{0.307 \cdot (1338.32 - 996.65)} \cdot 100 = 81.031\%$$

Table 4. Calculation results.

Parameter	Without fins	4 fins	6 fins	8 fins	22 fins
Efficiency, %	80,9	81,031	81,313	81,437	81,439
Hub shear stress, Pa	107,687	90,061	88,865	88,706	88,694
h_k, kJ/kg	1061,5	1061.47	1060,5	1060,02	1059.9

The following calculation includes a radial turbine with separator blades with a separator blade length b / B = 0.7, as well as fins on the entire surface of the wheel hub (**Figure 15**).

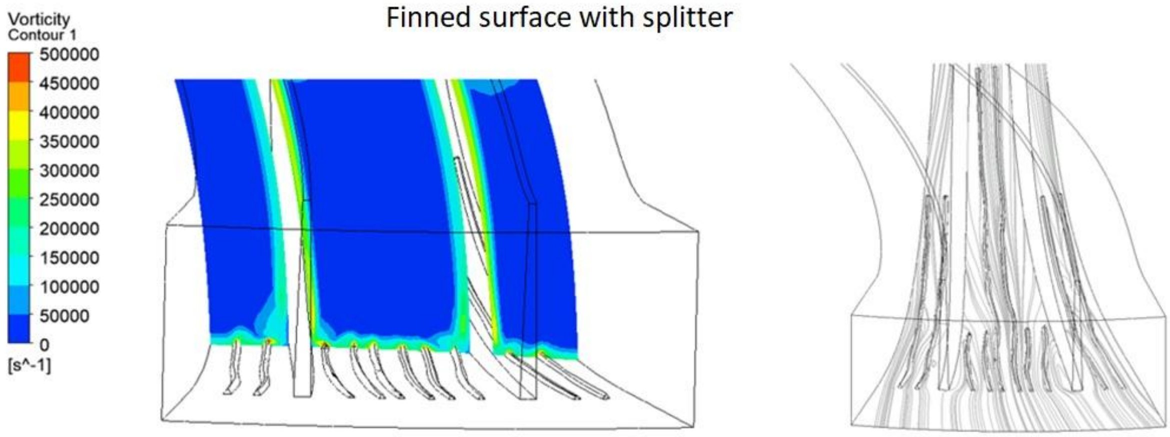

Figure 15. Vorticity diagram in a channel with splitters and fins, flow lines on the hub.

Based on the calculation results, the minimum value of wall shear stress at the hub surface was obtained, which is equal to 79.57 Pa. The maximum value of internal relative efficiency is 82.2% shows in (**Figure 16**).

The results of flow simulation in a radial turbine show that the configuration with fins and splitters has the highest internal relative efficiency of 82.2%. Among the configurations with splitters, the best result was achieved with splitters of relative length 0.7, with an efficiency of 81.75%. Adding an inter-tier partition without splitters improves efficiency by 0.8% by reducing velocity field unevenness. However, adding splitters to a two-tier radial wheel increases velocity field unevenness, creating a stagnation zone that reduces efficiency. The best result with fins was achieved with a fully finned surface, with an internal relative efficiency of 81.44%, indicating a minimal stagnation zone area near the wheel hub.

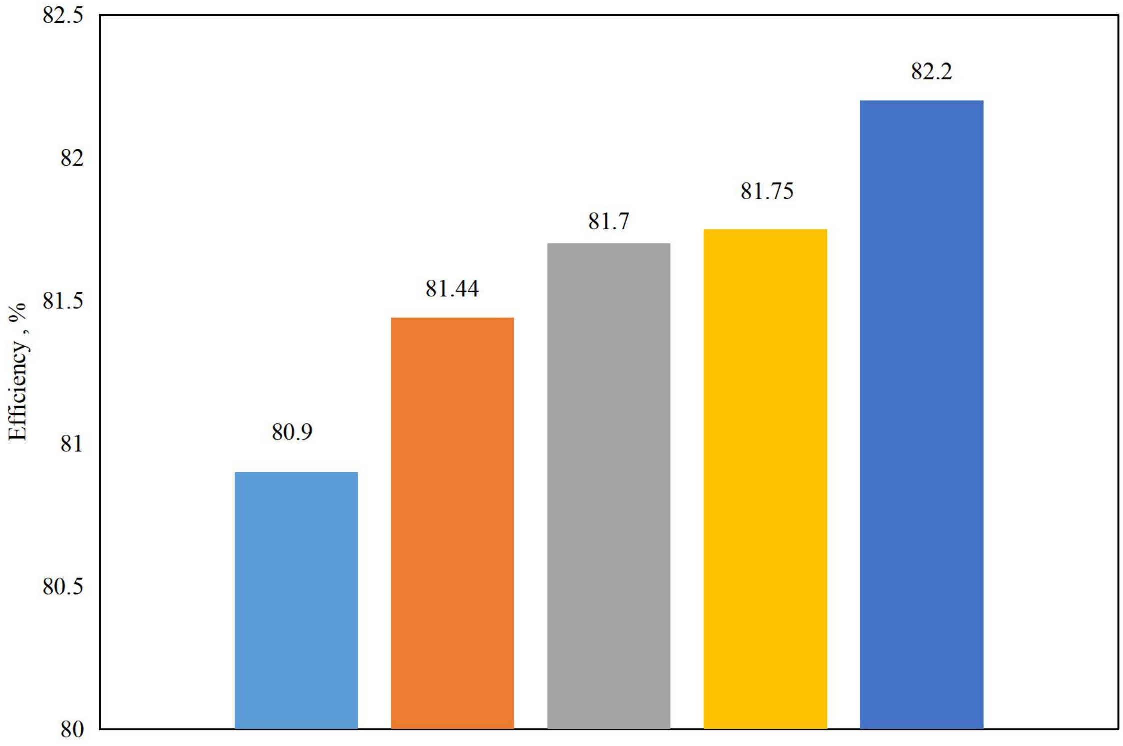

Figure 16. Internal relative efficiency of the flow path of a radial turbine of various design versions. Without Splitters & Fins (80.9%), Only with Fins (81.44%), Inner-tier partition (81.7%), Only with Splitter (81.75%) and With Splitters & Fin (82.2%).

5. Conclusion

The paper focuses on developing new solutions to enhance the aerodynamic performance of the radial turbine and the efficiency of the Capstone C30 micro-GTU by incorporating a cycle air cooling system and flow control systems. Key findings include:

Flow control methods in the blade channels of the radial turbine yield the following results:

- Using splitters with a relative length of 0.7 increases internal relative efficiency from 80.9% to 81.75% by dividing the main peripheral vortex.
- Implementing triangular root fins (0.1 mm high, 1 mm pitch, 22 pieces) enhances efficiency from 80.9% to 81.44% by reducing root flow overflow.
- Adding an inter-tier partition without splitters improves internal relative efficiency from 80.9% to 81.7% by minimizing flow transfer to the periphery and reducing velocity field unevenness.
- A finned turbine configuration with splitters of relative length 0.7 achieves the highest internal relative efficiency of 82.2%.

Overall, these advancements contribute to improved turbine performance and efficiency.

Author Contributions

For research articles with several authors, a short paragraph specifying their individual contributions must be provided. The following statements should be used “Conceptualization, SKO and MMS; methodology, MMS; software, ANB.; validation, SKO, VPS and IAM; formal analysis, MMS; investigation, MMS; resources, ANB; data curation, ANB.; writing—original draft preparation, ANB; writing—review and editing, MMS; visualization, MIA; supervision, SKO; project administration, IAM; funding acquisition, SKO. All authors have read and agreed to the published version of the manuscript." Authorship must be limited to those who have contributed substantially to the work reported.

Acknowledgment

This study conducted by Moscow Power Engineering Institute was financially supported by the Ministry of Science and Higher Education of the Russian Federation (project No. FSWF-2023-0014, contract No. 075-03-2023-383, 2023/18/01).

Conflict of interest

The authors declare no conflict of interest.

References

1. Popova Svetlana Nikolaevna, Potekhina Nina Vasilievna Prospects and Limitations of Distributed Energy Development in the Russian Electricity Market // Society: Politics, Economics, Law. 2016. No. 12. URL: https://cyberleninka.ru/article/n/perspektivy-i-ogranicheniya-razvitiya-raspredelennoy-energetiki-na-elektroenergeticheskom-rynke-rossii (date of access: 15.10.2022).
2. Wendland L. E., Pribylov V. G., Borisov Yu. A. Testing the C30 Capstone unit on gas fuel // Science City Science Production Society. - 2018. - No. 2. - P. 74-79.
3. Capstonepowersolutions.co.uk. (2023). Our Products – Capstone Power Solutions. [online] Available at: https://capstonepowersolutions.co.uk/our-products [Accessed 28 Nov. 2024].
4. Ventura CAM et al. Preliminary design and performance estimation of radial inflow turbines: an automated approach //Journal of Fluids Engineering. – 2012. – T. 134. – No. 3.
5. Hellstrom F., Fuchs L. Effects of inlet conditions on the turbine performance of a radial turbine //Turbo Expo: Power for Land, Sea, and Air. – 2008. – T. 43161. – S. 1985-2001.
6. Walsh M. Turbulent boundary layer drag reduction using riblets //20th aerospace sciences meeting. – 1982. – P. 169.
7. Oleksandr Liaposhchenko, Pavlenko, I., Katarina Monkova, Maryna Demianenko and Oleksandr Starynskyi (2019). Numerical Simulation of Aeroelastic Interaction Between Gas-Liquid Flow and Deformable Elements in Modular Separation Devices. [online] doi:https://doi.org/10.1007/978-3-030-22365-6_76.
8. Thijs van Druenen and Blocken, B. (2024). CFD simulations of cyclist aerodynamics: Impact of computational parameters. Journal of Wind Engineering and Industrial Aerodynamics, 249, pp.105714–105714. doi:https://doi.org/10.1016/j.jweia.2024.105714.
9. Chipongo, K., Khiadani, M. and Sookhak Lari, K. (2020). Comparison and verification of turbulence Reynolds-averaged Navier–Stokes closures to model spatially varied flows. Scientific Reports, 10(1). doi:https://doi.org/10.1038/s41598-020-76128-9.
10. Yaniel Garcia Lovella, Idalberto Herrera Moya, Jayasuriya, J. and Blondeau, J. (2024). Reynolds-average Navier-Stokes turbulence models assessment: A case study of CH4/H2/N2-air reacting jet. Heliyon, [online] 10(5), pp.e26956–e26956. doi:https://doi.org/10.1016/j.heliyon.2024.e26956.
11. Khopkar, A., Aubin, J., Rubio-Atoche, C., Xuereb, C., Le Sauze, N., Bertrand, J. and Ranade, V.V. (2004). Flow Generated by Radial Flow Impellers: PIV Measurements and CFD Simulations. International Journal of Chemical Reactor Engineering, 2(1). doi:https://doi.org/10.2202/1542-6580.1146.
12. Gebrewold, D.L., Riedelbauch, S. and Dribssa, E. (2024). Hydraulic design of a very low head axial turbine for clean energy option at Tana-Beles sugar irrigation canal in Ethiopia. Energy for Sustainable Development, [online] 83, p.101556. doi:https://doi.org/10.1016/j.esd.2024.101556.
13. Marsan, A. and Moreau, S. (2015). Analysis of the Flow Structure in a Radial Turbine. [online] Euroturbo. Available at: https://www.euroturbo.eu/publications/proceedings-papers/etc2015-207/ [Accessed 28 Nov. 2024].
14. Shahid, S., Hasan, A.Q., Sham Dol, S., S. Gadala, M. and Aris, M.S. (2021). Effects of Near-Wall Vortices on Wall Shear Stress in a Centrifugal Pump Impeller. WSEAS TRANSACTIONS ON FLUID MECHANICS, 16, pp.37–47. doi:https://doi.org/10.37394/232013.2021.16.5.
15. Birk, L. (2019). Wall Shear Stress in the Boundary Layer. [online] doi:https://doi.org/10.1002/9781119191575.ch11.